Published OnlineFirst July 28, 2006; DOI: 10.1158/1541-7786.MCR-06-0111

Histone Deacetylase Inhibitors (HDI) Cause DNA Damage in Leukemia Cells: A Mechanism for Leukemia-Specific HDI-Dependent Apoptosis?

Terry J. Gaymes,[1] Rose Ann Padua,[1,2] Marika Pla,[2] Stephen Orr,[1] Nader Omidvar,[3] Christine Chomienne,[2] Ghulam J. Mufti,[1] and Feyruz V. Rassool[1,4]

[1]Department of Haematological Medicine, Leukemia Sciences Laboratories, The Rayne Institute, GKT School of Medicine, Denmark Hill campus, London, United Kingdom; [2]Institut National de la Sante et de la Recherche Medicale U718, Institût Universitaire d'Hématologie, Hôpital Saint-Louis, Paris, France; [3]School of Biosciences, Cardiff University, Cardiff, United Kingdom; and [4]Department of Radiation Oncology, University of Maryland School of Medicine, Baltimore, Maryland

Abstract

Histone deacetylase inhibitors (HDI) increase gene expression through induction of histone acetylation. However, it remains unclear whether increases in specific gene expression events determine the apoptotic response following HDI administration. Herein, we show that a variety of HDI trigger in hematopoietic cells not only widespread histone acetylation and DNA damage responses but also actual DNA damage, which is significantly increased in leukemic cells compared with normal cells. Thus, increase in H2AX and ataxia telangiectasia mutated (ATM) phosphorylation, early markers of DNA damage, occurs rapidly following HDI administration. Activation of the DNA damage and repair response following HDI treatment is further emphasized by localizing DNA repair proteins to regions of DNA damage. These events are followed by subsequent apoptosis of neoplastic cells but not normal cells. Our data indicate that induction of apoptosis by HDI may result predominantly through accumulation of excessive DNA damage in leukemia cells, leading to activation of apoptosis. (Mol Cancer Res 2006;4(8):563–73)

Introduction

Histone deacetylase inhibitors (HDI) abrogate the action of histone deacetylases, a group of enzymes that control global chromatin architecture through histone modification. In turn, inhibition of histone deacetylation results in chromatin relaxation and increased access of transcriptional elements to promoters, leading to enhanced gene activity (1-3). Leukemias are seen as particularly good candidates for HDI therapy. These agents result in apoptosis of cancer cells *in vivo* and are now undergoing phase I/II clinical trials (4). In these diseases, specific oncogenic fusion proteins can recruit histone deacetylases to the promoters of their target genes and these events may constitute major steps in leukemogenesis (5).

Recently, it has been suggested that chromatin changes induced by HDI can directly activate the DNA damage pathway (6). Activation of ataxia telangiectasia mutated (ATM) kinase seems to be an initiating event in cellular responses to irradiation. ATM activation is not dependent on direct binding to DNA strand breaks but may result from changes in the structure of chromatin (6).

It has been widely reported that HDI induces $p21^{waf}$ and/or Fas ligand binding that could ultimately result in apoptosis of tumor cells (7). Several HDI, including valproic acid and suberoylanilide hydroxamic acid, show antileukemic activities correlating with overexpression of the cell cycle inhibitor $p21^{waf}$ (8, 9). Recently, it has been reported that, in addition to $p21^{waf}$, HDI induce tumor necrosis factor–related apoptosis-inducing ligand (Apo2L, TNFSF10) by directly activating the TNFSF10 promoter, thereby triggering tumor-selective death signaling in acute myeloid leukemia (AML) cell lines, murine acute promyelocytic leukemia (APL) cells *in vivo*, and cells from patients with AML (10, 11).

Herein, we have investigated the alternative possibility that HDI might induce actual DNA damage that then triggers apoptotic events. We find that, within minutes of HDI treatment, DNA damage is detected in the form of regions of ssDNA that is coincident with acetylation of histone H4. Importantly, apoptosis, as detected by caspase-3 and poly(ADP-ribose) polymerase cleavage, is only detected some hours following HDI treatment *in vitro* and *in vivo*. Furthermore, abrogating the expression of key molecules in the DNA damage and repair response, such as H2AX and ATM, leads to an accumulation of DNA damage and accelerated apoptosis in HDI-treated cells. Importantly, leukemic cells that overexpress BCL2 still show DNA damage, while apoptosis is abolished. Thus, although apoptosis may be triggered by HDI, this is likely in some instances to occur downstream of DNA-damaging events.

Received 4/25/06; revised 6/19/06; accepted 6/21/06.
Grant support: Elimination of Leukemia Fund (United Kingdom), Fondation de France, and Institut National de la Sante et de la Recherche Medicale.
The costs of publication of this article were defrayed in part by the payment of page charges. This article must therefore be hereby marked advertisement in accordance with 18 U.S.C. Section 1734 solely to indicate this fact.
Note: Supplementary data for this article are available at Molecular Cancer Research Online (http://mcr.aacrjournals.org/).
Requests for reprints: Feyruz V. Rassool, Department of Radiation Oncology, University of Maryland School of Medicine, 655 West Baltimore Street, BRB 7-009, Baltimore, MD 21201-1509. Phone: 410-706-5337; Fax: 410-706-3000. E-mail: frassool@som.umaryland.edu

doi:10.1158/1541-7786.MCR-06-0111

Published OnlineFirst July 28, 2006; DOI: 10.1158/1541-7786.MCR-06-0111

Results

HDI have been shown to differentially induce apoptosis in cancer and leukemic cells (10, 11). However, the mechanism underlying the action of HDI is still not entirely understood. We examined the possibility that HDI might actually induce DNA damage and then trigger apoptotic pathways. We first determined the relationship of acetylated histone H4 and phosphorylation of H2AX in normal and leukemic cells following HDI treatment. We first found that addition of HDI to normal and leukemic cells results in histone acetylation and rapid induction of variant histone H2AX phosphorylation on Ser^{139}. This DNA damage event signals for DNA repair in response to double-stranded breaks (DSB; refs. 12, 13). The AML cell line HL60 and normal interleukin-2-stimulated peripheral blood lymphocytes (PBL) in culture were treated with varying concentrations of trichostatin A, sodium butyrate, or the novel HDI apicidin for 24 hours. Administration of trichostatin A (300 nmol/L) resulted in phosphorylation of H2AX in HL60 (Fig. 1A) and, to a much lesser extent, normal PBL (Fig. 1B). H2AX phosphorylation occurred by 3 minutes (0.05 hour), peaked at 30 minutes (0.5 hour), and was still evident at 24 hours in leukemia cells. The timing of this change corresponded to concomitant increases in the acetylation of histone H4 (Fig. 1A and B) that could also be shown on chromatin fibers (Fig. 3A). Treatment of HL60 with apicidin (1 μmol/L; Fig. 1C) and sodium butyrate (1 mmol/L; Supplementary Fig. S1A) also resulted in H2AX phosphorylation at 10 minutes that was also concomitant with enhancement of histone H4 acetylation. Importantly, we observed the same results in primary cells from AML patients (n = 4; Fig. 1D), the APL cell line NB4 (Supplementary Fig. S1B), and the chronic myeloid leukemia K562 cell line (Supplementary Fig. S1C).

The phosphorylation of the protein kinase ATM is an important mediator of the DNA damage response (14). In accordance with the work of Bakkenist and Kastan, we show increased phosphorylation of ATM in HL60 cells treated with trichostatin A. This phosphorylation peaks at 10 minutes after drug administration and disappears over 8 hours (Fig. 1E).

As noted previously, HDI have been shown to induce apoptosis in leukemic cells and this may be the underlying mechanism most important to the antitumor effects of these drugs (4). Consistent with this notion, although there was background apoptosis in our leukemic cell lines, using flow cytometry, we saw distinct G_2-M arrest at 24 hours, and this was followed by a massive increase in a sub-G_1 peak, indicating a profound apoptosis by 48 hours in our leukemic cell lines treated with HDI (data not shown). However, the onset of apoptosis, as marked by the cleavage of caspase-3 and poly(ADP-ribose) polymerase, begins as early as 4 hours after HDI administration in HL60 cells and well after the appearance of increased histone acetylation, activation of H2AX (Fig. 1A, C, and D; Supplementary Fig. S1A, B, and D), and ATM phosphorylation (Fig. 1E). Importantly, the DNA damage we observed in leukemic cells following HDI is not an early manifestation of apoptosis, because K562 cells stably transfected with antiapoptotic BCL2 (Fig. 2A) inhibit caspase cleavage (Fig. 2B and C) following HDI treatment but still induce DNA damage as measured by γH2AX (Fig. 2D). We also note that BCL2 transfectants treated with HDI show more DNA damage foci at an earlier time point following HDI treatment than K562 controls (Table 1). In addition, overall histone acetylation is not associated per se with apoptosis induced by other non-HDI agents. Thus, addition of the proapoptotic agent staurosporine (1 μmol/L) also resulted in H2AX phosphorylation at 240 minutes but with no concomitant increase in histone H4 acetylation in HL60 (Fig. 1G) and normal PBL (Fig. 1H).

All of this data suggest that, specifically in leukemic cells, therapeutic doses of HDI cause DNA damage in association with the acetylation of histone proteins and that apoptosis subsequently follows these events. To confirm that HDI caused DNA damage in leukemic cells, we searched directly for evidence of DNA damage on chromatin fibers using an established assay for DNA damage that relies on the fact that an anti–bromodeoxyuridine (BrdUrd) antibody can only detect BrdUrd incorporated into DNA when it is in ssDNA form. Raderschall et al. revealed these regions of damage in cells following treatment with DSB-inducing agents, such as etoposide and ionizing radiation (15-17). Their data suggested that ssDNA regions form immediately following DSB induction presumably due to processing of the DNA termini as a prelude to DSB repair (15-17). Analyzing chromatin fibers from HL60 cells by this assay, we saw that treatment of cells with HDI induced DNA damage that colocalized with acetylated histone H4 (Fig. 3A). As early as 10 minutes after HDI administration, an increase in DNA damage was detected. Thus, with time after HDI treatment (10 minutes to 2 hours), 50% to 80% of the chromatin fibers stained positive for acetylated histones and up to 73% of these colocalized with BrdUrd-positive ssDNA regions (Supplementary Table S1). In contrast, chromatin fibers from untreated HL60 cells (n = 3) showed that 7% stain positive for acetylated histones, and no colocalization of acetylated histones and BrdUrd was detected (Fig. 3A; Supplementary Table S1). These positive regions of DNA damage also colocalized with γH2AX on chromatin fibers (Fig. 3B). We found that both the number of fibers and the intensity of staining for both acetylated histones and BrdUrd and their colocalization increased with length of incubation of trichostatin A (data not shown). These data suggest that DNA damage follows or is at least concomitant with HDI-induced histone acetylation in HL60 cells. In contrast, we obtained data to suggest that DNA damage, in general, does not cause the global chromatin changes that are induced by treatment of cells with HDI. Thus, γ-irradiation of HL60 or normal PBL showed phosphorylation of H2AX less than 3 minutes after the return to culture, but this was not accompanied by any increase in overall histone H4 acetylation (Figs. 1F).

To further confirm that actual DNA damage responses were engendered by HDI treatment, we searched for key DNA repair factors that may be recruited to sites of DNA damage. We thus immunostained chromatin fibers from HL60 for acetylated histones and/or DNA damage followed by coimmunostaining for DNA repair proteins, such as Ku86 and DNA-dependent protein kinase catalytic subunit (DNA-PK). These proteins participate in one of the main pathways that repair DSB, nonhomologous end joining. We found that trichostatin A

Published OnlineFirst July 28, 2006; DOI: 10.1158/1541-7786.MCR-06-0111

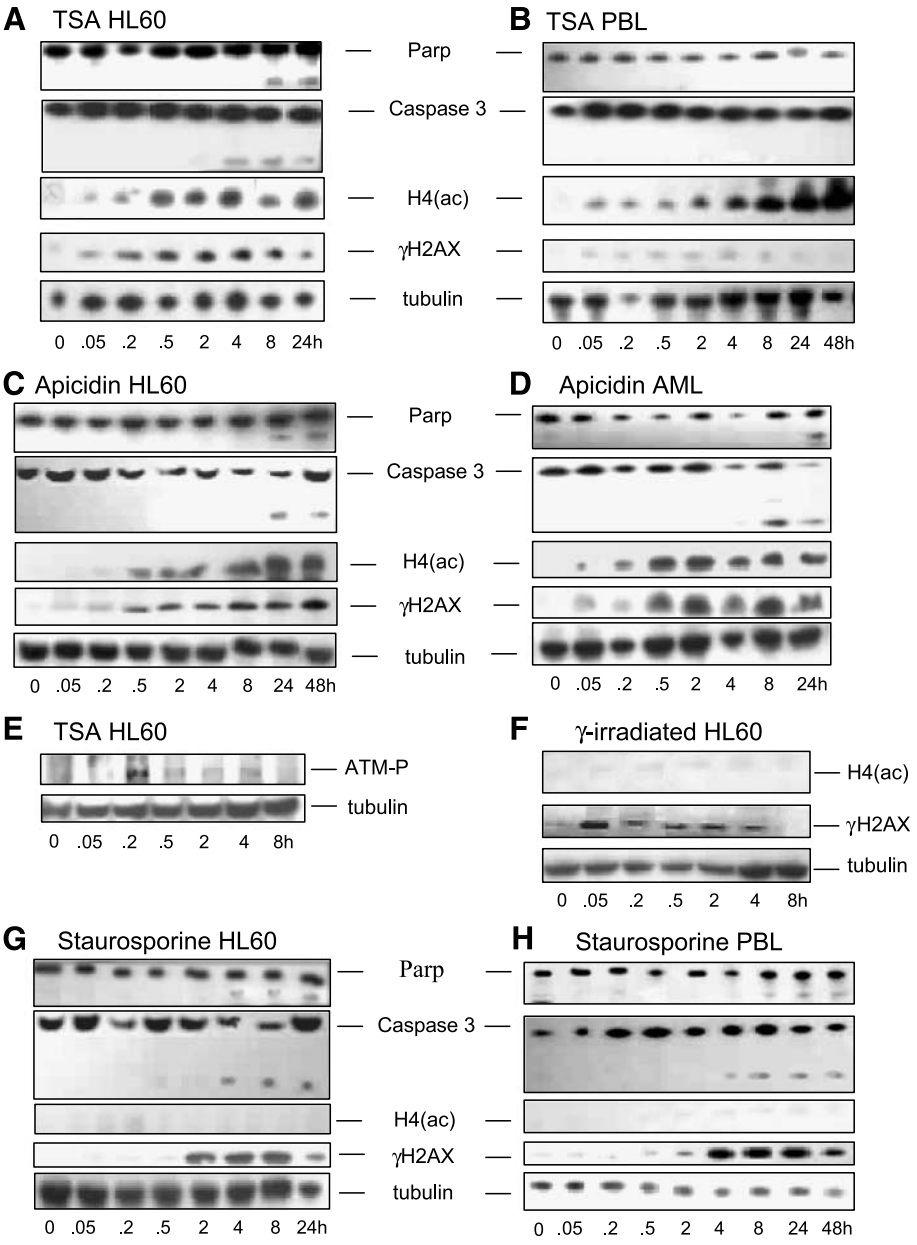

FIGURE 1. DNA damage and apoptosis responses to treatment of cells with HDI as analyzed by Western blotting. **A.** Trichostatin A (*TSA*; 300 nmol/L) was added to HL60 cells for 24 hours. **B.** Trichostatin A (300 nmol/L) was added to PBL for 48 hours. **C.** Apicidin (1 μmol/L) was added to HL60 cells for 48 hours. **D.** Apicidin (1 μmol/L) added to primary cycling AML cells for 24 hours. **E.** ATM phosphorylation measured in HL60 cells treated with trichostatin A (300 nmol/L) for 480 minutes. **F.** HL60 cells were γ-irradiated and returned to culture for 480 minutes. **G.** Staurosporine (1 μmol/L) was added to HL60 cells for 24 hours. **H.** Staurosporine (1 μmol/L) was added to PBL for 48 hours.

induces histone acetylation along the chromatin fiber in treated compared with untreated cells (Fig. 3A), and this acetylation colocalizes with Ku86 (Fig. 3C). Furthermore, the HDI-induced phosphorylation of H2AX colocalizes with another nonhomologous end joining repair factor, DNA-PK (Fig. 3D). All of these changes also colocalize with the ssDNA regions revealed by BrdUrd staining along the length of the chromatin fiber (Fig. 3A and B). Importantly, to confirm that this assay can detect DNA damage, we used chromatin fibers from γ-irradiated HL60 cells as a positive control and similar DNA damage to that generated by HDI treatment that colocalizes with DNA-PK (Fig. 3E) was seen.

Importantly, in normal PBL treated with HDI, Western blot analyses for phosphorylated H2AX showed a significant increase in γH2AX protein phosphorylation in leukemic versus normal cells (Fig. 1B). Furthermore, we also saw evidence for DNA damage on chromatin fibers from normal PBL, but the amount of damage seemed considerably less than that induced in leukemic cells (Fig. 4A). The formation of γH2AX foci in nuclei following DNA damage has been used as a sensitive measure of DSB damage rather than measurement by Western blot analysis (18, 19). To assess the differences in DNA damage more quantitatively, we examined γH2AX foci formation in normal PBL and HL60 cells following HDI treatment. We showed that untreated HL60 cells contain low levels of γH2AX foci, whereas no foci are observed in normal PBL. HDI treatment results in a large increase in foci in HL60 cells compared with DNA damage in

Published OnlineFirst July 28, 2006; DOI: 10.1158/1541-7786.MCR-06-0111

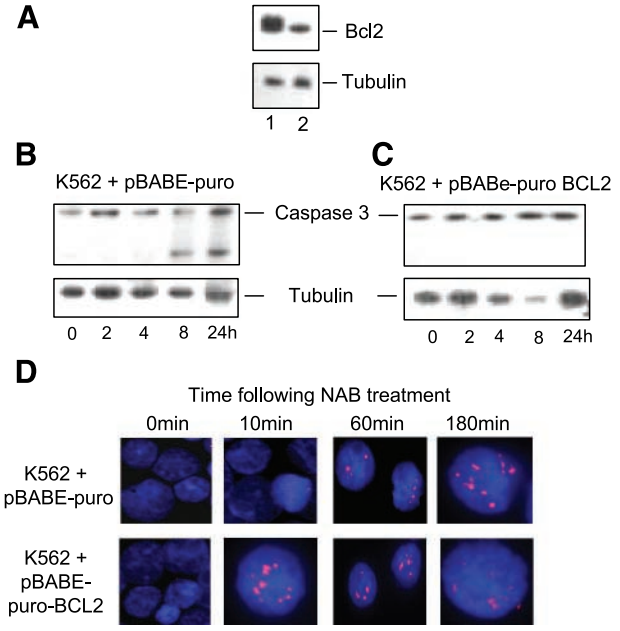

FIGURE 2. Effect of HDI on leukemic cells stably transfected with BCL2. **A.** Western blot showing expression of BCL2 in K562 cells after transfection of pBABE-puro-BCL2. Lane 1, K562 stably transfected with pBABE-puro-BCL2; lane 2, K562 stably transfected with the empty vector only. **B.** Sodium butyrate (1 mmol/L) was added to K562 cells stably transfected with BCL2 for 24 hours. **C.** Sodium butyrate (1 mmol/L) was added to K562 stably transfected with empty vector pBABE-puro for 24 hours. **D.** Immunostaining for γH2AX of nuclei (DAPI; *blue*) from K562 cells stably transfected with BCL2 or with the empty vector pBABE-puro and treated with sodium butyrate (*NAB*). Cytospins were prepared at the stated time points following incubation with sodium butyrate and immunoprobed for γH2AX (*red*). Representative K562 nuclei.

normal PBL (Fig. 4B; Table 1). Importantly, γH2AX foci in HL60 cells persist for a longer time (>3 hours) following HDI treatment compared with normal cells (Fig. 4B). Similar results were observed for NB4 leukemic cell lines using trichostatin A, sodium butyrate, and apicidin (Fig. 4C; Tables 1 and 2). Taken together, all of our results in cell culture indicate that HDI results in increased and prolonged DNA damage in leukemic cells compared with normal PBL.

To determine whether the increased DNA damage and apoptosis we have reported in leukemic cells following treatment with HDI *in vitro* also occurs *in vivo*, we used an APL transplantable mouse model (20). One of the advantages of using this mouse model is that the controls will have the same genetic background as the APL mice. Blast cells (10^4) were isolated from spleens of APL mice and injected i.v. into 6- to 8-week-old naive syngeneic animals (20), which was the minimum dose sufficient to induce leukemia. APL mice and their syngeneic FVB/N controls were injected on day 11 after APL injection with trichostatin A for 4 hours and extracts were prepared from spleen cells. In chromatin fibers stained for γH2AX, 60% of APL cells treated with trichostatin A showed DNA damage versus 20% from untreated cells ($n = 3$; data not shown). Importantly, chromatin fibers from normal FVB/N mice treated with trichostatin A showed smaller increases in DNA damage (7% from untreated cells versus 13% from treated cells; $n = 3$) than splenic APL cells from these mice. We were also able to show selective apoptosis of APL mice spleen cells with trichostatin A (Fig. 4D). Trichostatin A had little effect on normal FVB/N mouse caspase cleavage. FVB/N and APL cells treated with arsenic trioxide (As_2O_3) show apoptosis as shown previously (21-23). Thus, the amount of DNA damage and apoptosis were dramatically increased in leukemic versus normal cells with trichostatin A treatment *in vivo* as has been shown *in vitro*.

To determine whether there is a distinct functional link between the key initiating DNA damage repair factors and HDI, we examined leukemic cells in which expression of these proteins is abrogated. H2AX is an early chromatin modification that demarcates DSB (24, 25). We examined apoptosis and DNA damage in leukemia cell lines (K562, HL60, and NB4) silenced for H2AX following HDI treatment. In cells where H2AX expression is knocked down to ~20% of normal (Fig. 5A), there is a faster onset of caspase cleavage compared with HDI-treated, unsilenced counterparts. Thus, in apicidin- and trichostatin A–treated H2AX-silenced HL60 cells, caspase cleavage occurs at 120 minutes (Fig. 5B and C), whereas in HDI-treated control cells caspase cleavage is seen at 240 minutes (Fig. 1A and C). Early onset of apoptosis is also seen with sodium butyrate–treated, H2AX-silenced HL60 and K562 (Supplementary Fig. S2A and B) compared with unsilenced controls (Supplementary Fig. S1A and D). Furthermore, measurement of BrdUrd-positive ssDNA damage in HDI-treated leukemic cells silenced for H2AX showed that foci numbers are increased and seem to be sustained for a longer period of time compared with control small interfering RNA (siRNA)–treated cells (Fig. 5D; Table 3).

To confirm the altered DNA damage response following HDI treatment with γH2AX silencing, we examined cells null for another key early DNA damage response gene, ATM (GM5849). We find, as with H2AX silencing, that ATM-null cells show caspase cleavage at 2 hours following sodium butyrate treatment, whereas HDI-treated control fibroblasts show no apoptosis (GM00637; Fig. 5F and G). In addition, HDI-treated $ATM^{-/-}$ cells show increased γH2AX foci compared with control HDI-treated fibroblasts (Fig. 5E; Table 4).

Cancer cells exhibit defective checkpoints at all phases of the cell cycle (26). One mechanism that may explain the DNA damage that can occur through the alteration of chromatin structure or function induced by HDI treatment is if it occurs during DNA replication. If the DNA damage caused by HDIs is dependent on DNA replication, then wild-type cells because of intact DNA damage checkpoints might arrest in response to HDI-induced chromatin changes in S phase, thus showing no (or low levels of) DNA damage, whereas tumor cells might fail to effectively arrest and exhibit more DNA breakage. We therefore determined at which stage of the cell cycle DNA damage occurs in leukemic cells following HDI treatment using flow cytometry. Figure 6A shows that addition of 1 mmol/L sodium butyrate to HL60 for 30 minutes shows a predominant increase in γH2AX fluorescence in G_1, whereas sodium butyrate treatment for 90 minutes shows a shift in

Published OnlineFirst July 28, 2006; DOI: 10.1158/1541-7786.MCR-06-0111

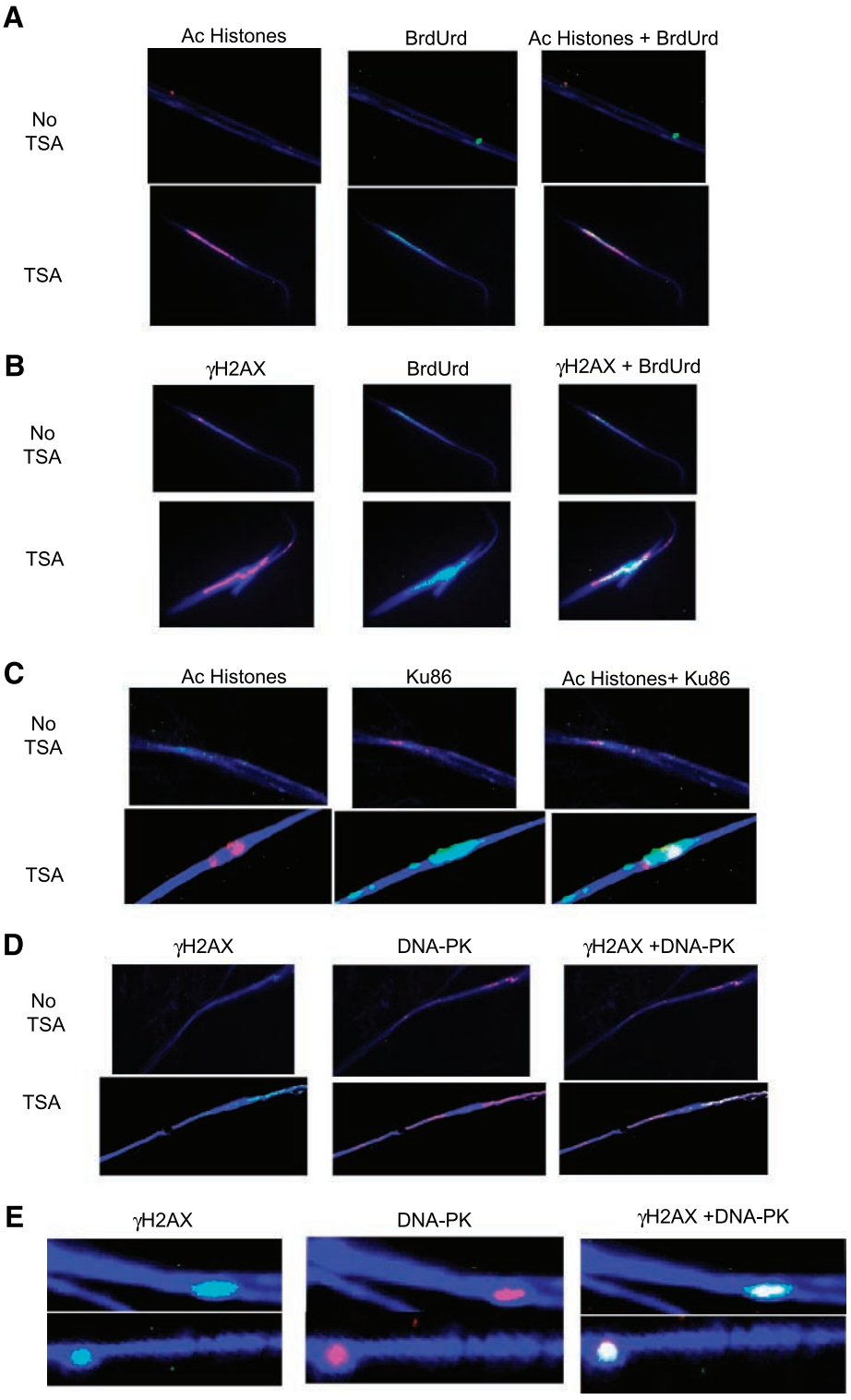

FIGURE 3. Trichostatin A induces DNA damage responses *in situ*. Coimmunostaining of chromatin fibers in HL60 cells. Consecutive images of single chromatin fibers stained for two different proteins followed by a merged image of the two staining patterns to detect colocalization. All chromatin fibers were counterstained with DAPI (*blue*). **A.** Costaining of fibers for DNA damage from cells grown for 30 hours in BrdUrd; fibers stained for acetylated (*Ac*) histone H4 (*red*) and BrdUrd (*green*) following treatment with trichostatin A (2 hours) and control untreated cells. Merged image shows regions of colocalization (*yellow*) **B.** Costaining of fibers for γH2AX (*red*) and BrdUrd (*green*) in trichostatin A (2 hours) and control untreated cells. **C.** Coimmunostaining of fibers for acetylated histone H4 (*red*) and nonhomologous end joining protein, Ku86 (*green*). **D.** Coimmunostaining of fibers for γH2AX (*green*) and DNA-dependent protein kinase catalytic subunit (*DNA-PK*; *red*). **E.** As a positive control, fibers were prepared from irradiated (1 Gy) HL60 cells. Fibers were coimmunostained for γH2AX (*green*) and DNA-dependent protein kinase catalytic subunit (*red*). Between 12 and 15 chromatin fibers were examined per experiment ($n = 3$).

γH2AX fluorescence toward G_1-S, S, and S-G_2 phases. In contrast, γ-irradiating HL60 cells results in a general increase in γH2AX fluorescence at all stages of the cell cycle. Thus, HDI treatment does not result in DNA damage exclusively in S-phase cells.

Discussion

It is widely accepted that HDI evoke antitumor activity through enhancement of specific antitumor gene transcriptional activity. However, HDI only increase transcription of between 5% and 10% of genes, whereas no definitive

Published OnlineFirst July 28, 2006; DOI: 10.1158/1541-7786.MCR-06-0111

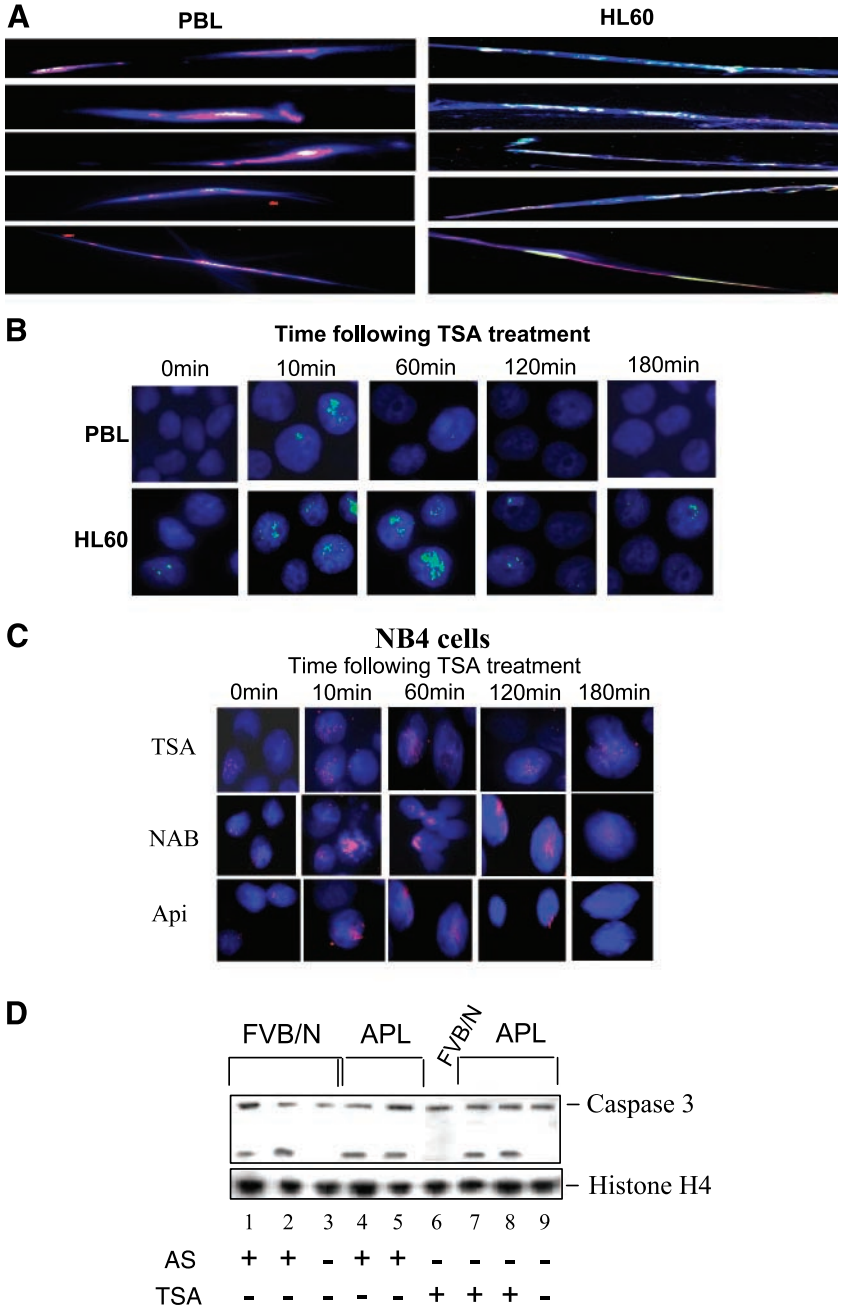

FIGURE 4. Leukemia cells are more susceptible to trichostatin A–derived DNA damage than normal cells. HL60 and normal PBL cells were treated with trichostatin A (300 nmol/L) for 1 hour and fixed with formaldehyde and chromatin fibers were prepared. **A.** Coimmunostaining of chromatin fibers for DNA damage from HL60 and PBL cells grown for 30 hours in BrdUrd and treated with trichostatin A (30 minutes). Five randomly captured images of chromatin fibers were stained for acetylated histone H4 (*red*) and BrdUrd (*green*) and then merged; yellow, regions of colocalization of acetylated histone H4 DNA damage. **B.** Immunostaining of nuclei (DAPI; *blue*) from trichostatin A–treated HL60 and PBL cells for γH2AX foci (*green*). Cytospins were prepared at the stated time points following incubation with trichostatin A and immunoprobed for γH2AX. Representative HL60 and PBL nuclei. **C.** Immunostaining of nuclei (DAPI; *blue*) of NB4 cells treated with trichostatin A, sodium butyrate, or apicidin (*Api*) for γH2AX foci (*red*). Cytospins were prepared at the stated time points following incubation with HDI and immunoprobed for γH2AX. Representative NB4 nuclei. **D.** Caspase cleavage Western blot analysis of APL and FVB/N mouse cells treated previously with trichostatin A. Positive controls are mice treated with As_2O_3 (*AS*), which cause apoptosis in FVB/N and APL cells. Lane 1, FVB/N + As_2O_3; lane 2, FVB/N; lane 3, FVB/N + As_2O_3; lane 4, APL + As_2O_3; lane 5, APL + As_2O_3; lane 6, FVB/N + trichostatin A; lane 7, APL + trichostatin A; lane 8, APL + trichostatin A; lane 9, APL.

antitumor gene activity has been attributed to HDI (27). It is thus conceivable that HDI exert their apoptotic properties by alternative means. We have shown here that in hematopoietic cell lines, primary cells, and mouse models a variety of HDI induce DNA damage and repair responses but result in significantly increased DNA damage in leukemic cells compared with normal cells. This damage occurs following induction of histone acetylation, and apoptosis occurs some time thereafter. This increased DNA damage in leukemic cells may well determine why they respond differentially to HDI with apoptosis compared with normal cells. Although the low levels of DNA damage in normal PBL are repaired by 1 hour after HDI treatment, DNA damage is still detectable in leukemic cells after 3 hours. Thus, leukemic cells may exceed a threshold of DNA damage that can be repaired, triggering apoptosis. Thus, our data are consistent with those observed by others where trichostatin A has been shown to induce apoptosis differentially in leukemic APL cells compared with normal cells (10, 11).

Our results suggest that this HDI-induced DNA damage may possibly occur through changes in chromatin structure. In fact, we show that phosphorylation of H2AX, one of the first cellular

Published OnlineFirst July 28, 2006; DOI: 10.1158/1541-7786.MCR-06-0111

Table 1. Detection of Percentage of γH2AX Foci by Immunofluorescence following Trichostatin A Treatment

Time point (min)	HL60	NB4	PBL	K562 + BCL2	K562 + pBABE
0	8 ± 1	6 ± 1	0	0	0
10	56 ± 7	49 ± 4	28 ± 4	27 ± 4	9 ± 2
30	50 ± 5	55 ± 2	14 ± 6	32 ± 1	5 ± 1
60	41 ± 8	22 ± 6	9 ± 2	37 ± 8	3 ± 1
180	22 ± 3	11 ± 5	0	27 ± 6	0

NOTE: One hundred nuclei were counted for each time point ($n = 3$).

responses to the induction of DSB (24), occurs concomitant with acetylation of histones. Furthermore, DNA damage assays showed that γH2AX colocalizes with regions of ssDNA. Because strand breaks are shown within minutes of HDI treatment, we believe the mechanisms may be different from those breaks observed previously with HDI-induced differentiation, which evolve over much longer periods of treatment (28). The DNA damage response is important in maintaining genomic instability (24, 25). We show here that cells with siRNA "knockdown" of H2AX or cells that are null for ATM, key players in the DNA damage response, result in altered amounts of DNA damage and onset of apoptosis. This suggests that in leukemic cells treated with HDI these processes are intimately linked.

Although the mechanism(s) by which histone acetylation cause DNA damage is unclear, it is well established that HDI leads to increased acetylation of many nonhistone and nontranscription factor proteins, altering their structure and function, which seem to play a role in HDI-induced apoptosis (29). Alternatively, or perhaps concomitantly, HDI-specific decompaction of chromatin could expose regions of DNA to endogenous DNA-damaging agents, of which reactive oxygen species are one example (30). Interestingly, recent findings show that HDI treatment itself results in an accumulation of reactive oxygen species in transformed but not normal fibroblasts (31, 32). One possible explanation for the DNA damage coincident with alteration of chromatin structure or function is if it occurs during DNA replication (33, 34). If the DNA damage caused by HDIs is dependent on DNA replication, then wild-type cells might escape the damage induction because of a better ability to arrest in response to HDI-induced chromatin changes in S phase, whereas tumor cells might fail to effectively arrest and exhibit some DNA breakage. We find that treatment of HL60 cells with HDI shows a subtle shift in γH2AX fluorescence toward G_1-S, S, and S-G_2, whereas γ-irradiating HL60 cells results in a general increase in γH2AX fluorescence at all stages of the cell cycle. Thus, HDI treatment does not lead to DNA damage exclusively in S-phase cells. However, further quantitation of these cell cycle–specific populations with and without DNA damage will determine whether S-phase cells exhibit more DNA damage due to defective checkpoints in leukemias.

We find that unlike the effect in leukemic cells HDI causes low levels of DNA damage in normal hematopoietic cells, which is repaired within 1 hour. This differs from data in normal human diploid fibroblasts where HDI was found to disrupt chromatin without causing DNA damage (6). Thus, it is quite conceivable that HDIs do not induce DNA damage in normal fibroblasts but do induce low levels of damage in normal hematopoietic cells. Our data showing that malignant cells exhibit excessive damage after HDI treatment that remains unrepaired 3 hours after HDI treatment suggests that the DNA damage load may trigger apoptosis. Thus, the relatively tumor-specific effect of HDI would provide an argument for some therapeutic selectivity advantage.

In summary, we propose a model for the action of HDI resulting in chromatin changes that cause DNA damage. Leukemic cells sustain more DNA damage than normal cells. Increased transcription of many of the proapoptotic genes shown by others with HDI treatment (4) then could be explained as a consequence of increased levels of unrepaired DNA damage. This induction of excessive DNA damage and subsequent apoptosis may be the key elements underlying the antitumor effects seen in patients with HDI administration. Elucidation of the mechanisms by which histone acetylation actually leads to DNA damage will be most important from a biological standpoint and may give us even further insights into the specific effects of HDI in tumor cells.

Materials and Methods

Cell Culture

Myeloid leukemia cell lines HL60, K562, and NB4 were purchased from the American Type Culture Collection (c/o LGC Promochem, Middlesex, United Kingdom). These cell lines were cultured at 37°C (5% CO_2) in Dutch modified RPMI 1640 supplemented with 10% FCS, 4 mmol/L glutamine, and 1% penicillin/streptomycin (all purchased from Sigma-Aldrich Co. Ltd., Poole, United Kingdom). Normal SV40-transformed fibroblasts GM00637 and ATM-null SV40-transformed fibroblasts were purchased from National Institute of General Medical Sciences Human Genetic Cell Repository, Coriell Cell Repositories (Camden, NJ). PBL from normal subjects were prepared from heparinized blood using Hypaque-Ficoll (Sigma-Aldrich) gradients and cultured at 1×10^6/mL in RPMI 1640 supplemented with 10% FCS, 4 mmol/L glutamine, and 1% penicillin/streptomycin. PBL were stimulated by adding phytohemagglutinin (Sigma-Aldrich) for 48 hours, washed several times to remove phytohemagglutinin, and then cultured in 1 unit/mL interleukin-2 for a maximum of 14 days. Newly diagnosed and untreated myeloid leukemia patient samples were received from hematology clinics. Clinical diagnosis and

Table 2. Detection of Percentage of γH2AX Foci in NB4 Cells by Immunofluorescence following Treatment with Sodium Butyrate and Apicidin

Time point (min)	Sodium butyrate	Apicidin
0	10 ± 2	3 ± 1
10	60 ± 2	38 ± 3
30	49 ± 3	49 ± 2
60	32 ± 5	45 ± 3
180	10 ± 2	8 ± 1

Published OnlineFirst July 28, 2006; DOI: 10.1158/1541-7786.MCR-06-0111

cytogenetics analysis was made on each sample before primary cell harvesting using Hypaque-Ficoll gradients. The mononuclear fraction was isolated from 10 to 20 mL AML bone marrow aspirate. Cytospins of these fractions were examined morphologically after May-Grunwald Giemsa staining and revealed the presence of >95% of AML blasts ($CD34^+$). Primary cells were cultured at 1×10^6/mL in Iscove's modified Dulbecco's medium (Sigma-Aldrich) supplemented with 20% FCS, 4 mmol/L glutamine, and 1% penicillin/streptomycin. Cells were stimulated by adding 10 ng/mL stem cell factor (R&D Systems, Abingdon, United Kingdom), 10 ng/mL interleukin-6, and 10 ng/mL interleukin-3 and grown to a density of 1×10^6/mL for 5 days. Log-phase cells were treated with HDIs at concentrations used previously to elicit histone acetylation. γ-Irradiation of log-phase cells was done on ice in a Gammacell Cobalt 60 γ-irradiator at doses between 3 and 10 Gy (6.52 Gy/min). Cells were then returned to culture in fresh prewarmed medium for 10 minutes.

Reagents

Trichostatin A and sodium butyrate were purchased from Sigma-Aldrich and prepared in ethanol and PBS, respectively. Staurosporine, zVAD-fmk and apicidin (Calbiochem, Beeston, United Kingdom) were prepared in DMSO.

Plasmids and Antibodies

Rabbit polyclonal antisera raised against human and mouse Ku86, Ku70, DNA-dependent protein kinase catalytic subunit,

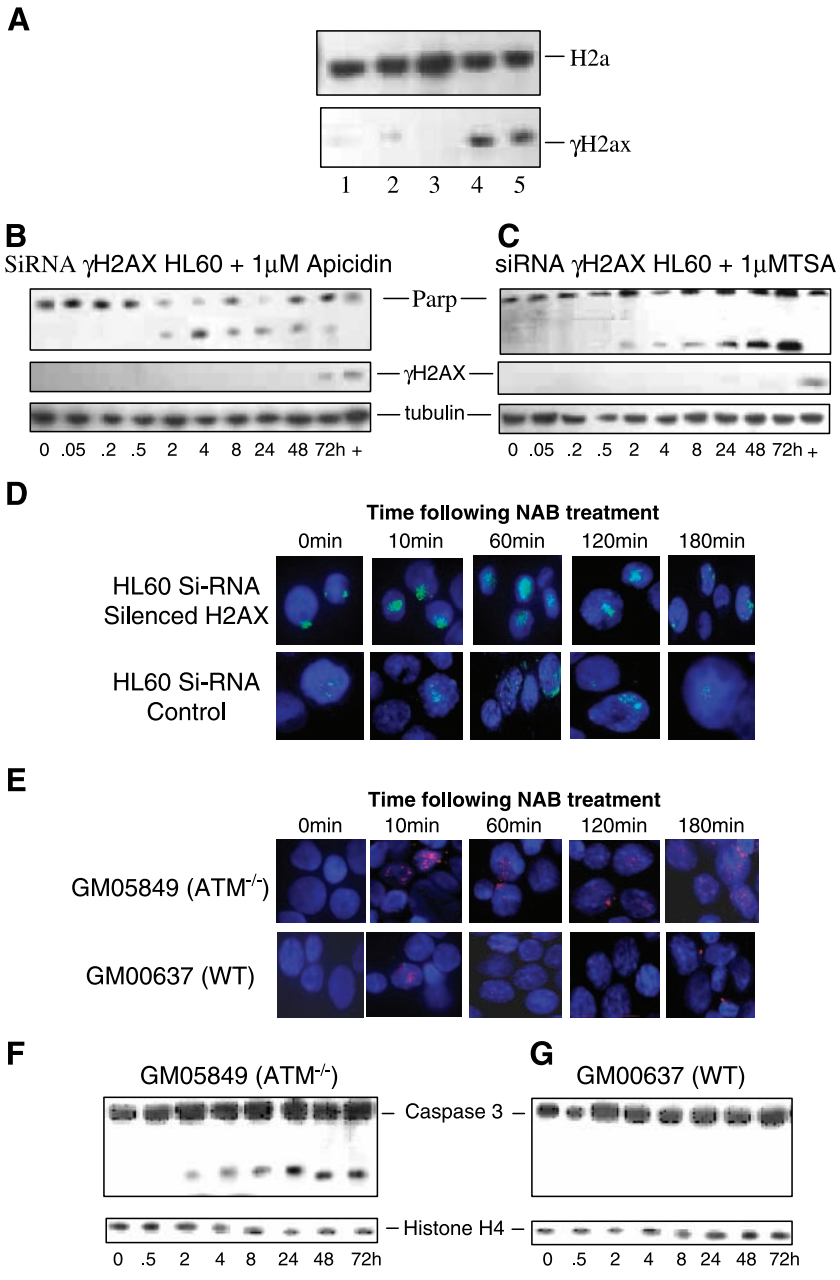

FIGURE 5. Effect of siRNA silencing of H2AX on HDI administration. **A.** Western blot analysis. Lane 1, untreated HL60 + H2AX siRNA; lane 2, γ-irradiated HL60 + H2AX siRNA; lane 3, trichostatin A–treated HL60 + H2AX siRNA; lane 4, γ-irradiated HL60 + scrambled siRNA; lane 5, trichostatin A–treated HL60 + scrambled siRNA. **B** and **C.** Western blot analysis of the effect of H2AX silencing on HDI-induced caspase cleavage in HL60: (**B**) apicidin for 72 hours and (**C**) trichostatin A for 72 hours. Lane +, 30-minute sample of γ-irradiated HL60. **D.** Immunostaining of nuclei (DAPI; *blue*) from sodium butyrate–treated, siRNA-silenced H2AX HL60 cells for BrdUrd-positive DNA damage foci (*green*). Cytospins were prepared at the stated time points following incubation with sodium butyrate and immunoprobed for BrdUrd. Representative HL60 nuclei. Sodium butyrate–treated HL60 were also transfected with scrambled siRNA to control for silencing. **E.** Immunostaining of nuclei (DAPI; *blue*) from sodium butyrate–treated, GM05849 ($ATM^{-/-}$) fibroblasts and wild-type (*WT*) GM00637 fibroblasts for γH2AX foci (*red*). Representative nuclei. **F** and **G.** Western blot analysis of the effect of sodium butyrate on $ATM^{-/-}$ fibroblast and wild-type fibroblast caspase cleavage: (**F**) GM05849 ($ATM^{-/-}$) for 72 hours and (**G**) GM00637 (wild-type) fibroblasts for 72 hours.

Published OnlineFirst July 28, 2006; DOI: 10.1158/1541-7786.MCR-06-0111

Table 3. Detection of Percentage of BrdUrd Foci in HL60 Cells by Immunofluorescence following siRNA Silencing of H2AX and Subsequent HDI Treatment

Time point (min)	siRNA H2AX	siRNA Control
0	21 ± 3*	15 ± 1
10	59 ± 6	49 ± 8
30	77 ± 8	58 ± 7
60	65 ± 9	20 ± 3
180	65 ± 2	7 ± 3

*Mean ± SD percentages of cells with BrdUrd foci (>5 foci per cell; $n = 3$).

caspase-3, poly(ADP-ribose) polymerase, tubulin, histone H4, and acetylated histone H4 were purchased from Serotec (Oxford, United Kingdom). Rabbit anti-γH2AX mouse anti-phosphorylated ATM (Ser^{1981}) was purchased from Upstate (Charlottesville, VA). Mouse anti-human BCL2 was purchased from BD Biosciences (Franklin Lakes, NJ).

Retroviral Infection

pBABE-puro empty vector and pBABE-puro-BCL2 (35) cDNA constructs were used in the generation of replication-defective amphotropic retrovirus by transient transfection of the Phoenix-Ampho packaging line (American Type Culture Collection). This was subsequently used to infect parental K562 line as described previously (36). In brief, RetroNectin (Takara Biochemicals, Takara Shiga, Japan)–coated 24-well plate wells were blocked with 1% bovine serum albumin and infection was carried out with 400 mL retroviral supernatant together with 1×10^5 cells at semilogarithmic growth phase in 1.5 mL culture medium. This was incubated overnight at 37°C, 5% CO_2 after which the infection procedure was repeated using fresh retroviral supernatant. Following infection, antibiotic selection was carried out in the presence of puromycin (2 mg/mL).

Western Blotting

Cell lysates (1×10^6 cells) from leukemic myeloid cells, PBL, and primary $CD34^+$ progenitor cells were prepared and resolved by SDS-PAGE (4-12% gradient gels; Invitrogen, Paisley, United Kingdom). Proteins were subsequently transferred to nitrocellulose membranes using electroblotting apparatus (Invitrogen). The membrane was blocked in 5% milk powder for 1 hour before overnight incubation at 4°C with primary antibody (1:1,000 dilution). Unbound antibody was removed with TBS containing 0.5% Tween 20. The membrane was then incubated with secondary antibody (horseradish peroxidase conjugated) for 1 hour at room temperature and washed four times in TBS containing 0.5% Tween 20, and detection was made using Enhanced Chemiluminescence Plus reagents (Amersham Pharmacia, Amersham, United Kingdom) according to the manufacturer's instructions.

Chromatin Fibers

Chromatin fibers were prepared from 1×10^6 cells according to the protocols of Raderschall et al. (15). However, the technique was modified to ensure subsequent detection of proteins binding at specific points of interest. Proteins were cross-linked to DNA by adding formaldehyde (1% final concentration) to the culture medium for 10 minutes at 37°C. Aliquots of 1×10^6 cells were cytospun onto glass slides and covered with 50 μL of 50 mmol/L Tris-HCl (pH 8), 1 mmol/L EDTA, and 0.1% SDS. After 1-minute incubation with this detergent solution, the chromatin was mechanically sheared on the slide with the aid of a glass coverslip, fixed in ethanol for 30 minutes at −20°C, and then rinsed in ice-cold acetone for up to 1 minute.

Immunofluorescence

Slides with chromatin fibers were incubated with blocking solution (10% bovine serum albumin/4× SSC/0.1% Tween 20) for 30 minutes at 37°C. Thereafter, slides were incubated in primary antibody diluted in blocking serum (1:10-1:50) and incubated for 30 minutes at 37°C. Slides were washed for 5 minutes in 4× SSC/0.1% Tween 20 and this was repeated twice more. The blocking step was repeated before slides were incubated in secondary antibody conjugated with fluorochromes diluted in blocking solution (1:200; Sigma-Aldrich) and subsequently washed as above. Cells were counterstained with 4′,6-diamidino-2-phenylindole (DAPI) for 1 minute and rinsed in PBS and coverslips were mounted in antifade solution ready for analysis. Slides were examined using an Olympus (London, United Kingdom) fluorescent microscope with DAPI/FITC/rhodamine triple-pass filters and images were captured using a charge-coupled camera and software (Smart capture VP, Digital Scientific Ltd., Cambridge, United Kingdom) and data were analysed (Quips XL, Vysis, Inc., Surrey, United Kingdom).

DNA Damage Studies

Cells were grown in 10 mmol/L BrdUrd (Sigma-Aldrich) for ~30 hours. Flasks were shielded from light. Thereafter, the cells were washed and placed in BrdUrd-free medium for 1 hour. Chromatin fibers were prepared from 1×10^6 cells according to the protocols of Raderschall et al (15). However, we modified the protocol to ensure subsequent detection of proteins binding at specific sites of interest. Proteins were cross-linked to DNA by adding formaldehyde (1% final concentration) to the culture medium for 10 minutes at 37°C before harvesting. Aliquots of 1×10^6 cells were cytospun onto glass slides and covered with 50 μL of 50 mmol/L Tris-HCl (pH 8), 1 mmol/L EDTA, and 0.1% SDS. After 1-minute incubation with the detergent solution, the chromatin was mechanically sheared on the slide with the aid of a glass coverslip and then fixed with methanol and acetone. Antibodies to BrdUrd will only detect

Table 4. Detection of Percentage of γH2AX Foci by Immunofluorescence following Sodium Butyrate Treatment

Time point (min)	$ATM^{-/-}$ GM05849	Wild-type control GM00637
0	0	0
10	39 ± 2	12 ± 1
30	52 ± 4	9 ± 3
60	29 ± 5	8 ± 1
180	21 ± 6	0

Published OnlineFirst July 28, 2006; DOI: 10.1158/1541-7786.MCR-06-0111

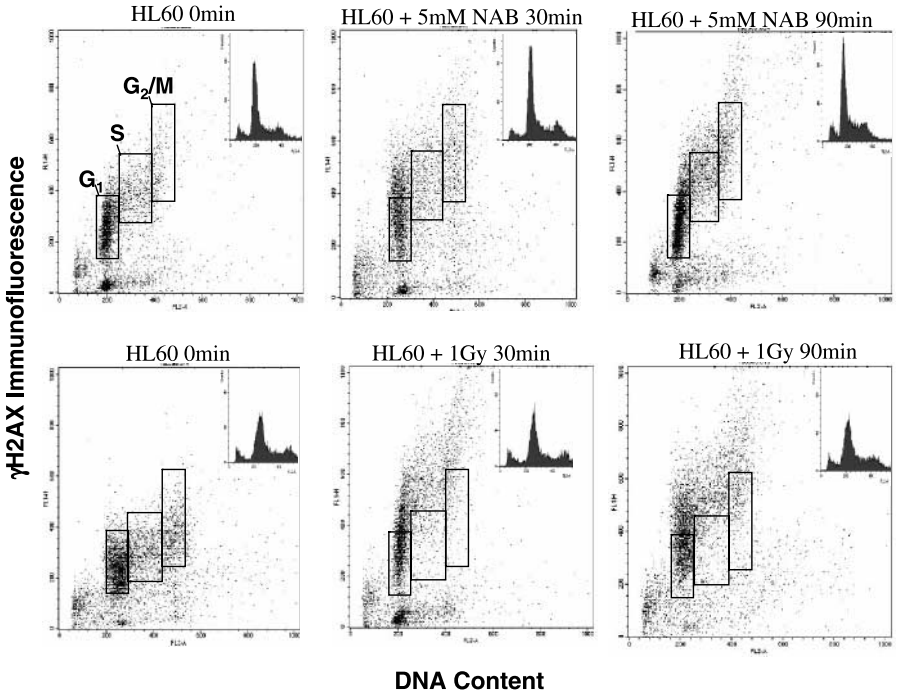

FIGURE 6. Bivariate (H2AX immunofluorescence versus DNA content) scatter plots showing untreated, 1 mmol/L sodium butyrate–treated, and γ-irradiated (1 Gy) HL60 cells at timed intervals. Solid boxes, outlines of cell populations of untreated cultures at G_1, S, and G_2-M phases. In treated cultures, cells exhibit increased fluorescence outside of these boxes with respect to the untreated sample. Insets, DNA content frequency histograms.

BrdUrd incorporation at ssDNA regions. Thus, this protocol is specific for the detection of regions of DNA damage.

Immunofluorescence for Flow Cytometry

After drug treatment, cells were fixed in 1% paraformaldehyde solution for 5 minutes at room temperature and then subsequently resuspended in 80% ethanol at −20°C overnight. Cells were then washed twice in wash solution (PBS/0.5% Tween 20/1% bovine serum albumin) and then incubated in 1% Triton X-100/10% bovine serum albumin for 30 minutes. Cells were washed again; thereafter, cells were resuspended in 100 μL anti-γH2AX diluted 1:50 in wash solution for 2 hours at room temperature. After further washings, the cells were then incubated in 100 μL anti-mouse IgG FITC conjugate (1:50) for 30 minutes at room temperature in the dark. Cells were counterstained with 40 μg/mL propidium iodide/1 mg/mL RNase for 30 minutes before fluorescence measurement. Green (FITC) and red (propidium iodide) fluorescence was measure using the appropriate filters on a FACSCalibur (Becton Dickinson, Franklin Lakes, NJ). Experiments were done in duplicate in at least three different experiments.

siRNA Silencing

siRNA duplexes were manufactured by Dharmacon (Dallas, TX). The sense strand for human H2AX was CAACAAGAAGACGCGAAUCdTdT. A control siRNA was synthesized with no complementarity to H2AX. Transfection of myeloid cell lines with siRNA was carried out using Oligofectamine (Invitrogen) according to the manufacturer's instructions. Cells (1×10^6) in 15 mL Opti-MEM, including 10% FCS (Invitrogen) per T75 culture flask (Sarstedt, Leicester, United Kingdom), was incubated 24 hours before transfection. siRNA (10 nmol/L) was added to 25 μL Oligofectamine and added to the cells in 4 mL fresh Opti-MEM. Four hours after transfection, 2.5 mL Opti-MEM containing 30% FCS was added to the flask. Seventy-two hours after transfection, cultures were subjected to irradiation (3 Gy) and returned to culture for 15 minutes or 300 nmol/L trichostatin A was added for 2 hours. Cells were then harvested for Western blot analysis. Multiple siRNA cultures were set up to make nuclear extracts.

Cell Cycle Analysis

HDI were added to log-phase cells for 72 hours. At the indicated times, 2×10^5 cell aliquots were taken and centrifuged at $400 \times g$ for 10 minutes. The supernatant was aspirated and 70% ethanol (at −20°C) was added and gently vortexed. The cell suspension was again centrifuged at $400 \times g$ for 10 minutes. The supernatant was aspirated and 1 mL staining solution (PBS + 5 ng FITC, 40 μg propidium iodide, 500 μg RNase) was added. Samples were analyzed using the FACScan flow cytometer (Becton Dickinson). To identify S-phase cells, log-phase cultures were pulsed with 10 mmol/L BrdUrd for 30 minutes before preparation of cytospins followed by denaturing DNA and immunostaining as described previously.

Animal Models

Transgenic mice using the human PML-retinoic acid receptor α cDNA were constructed previously in the FVB/N inbred strain of mice (20). This transgene contains a new amino acid generated by the fusion of PML with retinoic acid receptor α. The transplant model is established from 10^4 blast cells isolated from spleens of transgenic animals injected i.v. in 6- to 8-week-old naive syngeneic mice (20), which was the minimum dose sufficient to induce leukemia in ~3 weeks. Establishment of leukemia is assessed by the appearance of high leukocyte and low platelet

Published OnlineFirst July 28, 2006; DOI: 10.1158/1541-7786.MCR-06-0111

counts at around day 10 (ref. 20; Hemavet counter, CDC Technologies, Oxford, CT). Enlargement of organs and tissue section examination confirms the cause of death from APL (21). All procedures complied with European or national regulations. On day 14 after APL injection, trichostatin A (1 mg/kg) was given i.p. for 4 hours; on day 11 after APL injection, trichostatin A was given for 4 days and 4 hours was found to be sufficient to induce maximal misrepair. Spleen cells were harvested and assayed for misrepair and DNA damage after trichostatin A administration for 4 hours and for apoptosis after trichostatin A administration for 4 days. As positive controls, for apoptosis, mice were treated with As_2O_3. A stock solution of 330 mmol/L As_2O_3 was prepared by diluting the powder in 1 mol/L NaOH; then, a dilution in TBS was given by daily i.p. injection at the concentration of 5 μg/g mice for a period of 5 days.

Acknowledgments

We thank Murielle Reboul and Thi-Hai Phan for technical assistance, Michael Bishop and Scott Kogan (University of California at San Francisco, San Francisco, CA) for the APL mouse cells, Prof. Stephen Baylin (Johns Hopkins, Baltimore, MD) for critical evaluation of the article, and Richard L. Darley (Cardiff School of Medicine) for technical advice and assistance in creation of the BCL2-infected K562 stable cell lines.

References

1. Drummond DC, Noble CO, Kirpotin DB, Guo Z, Scott GK, Benz CC. Clinical development of histone deacetylase inhibitors as anticancer agents. Annu Rev Pharmacol Toxicol 2005;45:495–528.

2. Bhalla KN. Epigenetic and chromatin modifiers as targeted therapy of hematologic malignancies. J Clin Oncol 2005;23:3971–93.

3. Marks PA, Richon VM, Miller T, Kelly WK. Histone deacetylase inhibitors. Adv Cancer Res 2004;91:137–68.

4. Marks PA, Richon VM, Rifkind RA. Histone deacetylase inhibitors: inducers of differentiation or apoptosis of transformed cells. J Natl Cancer Inst 2000;92:1210–6.

5. Jones LK, Saha V. Chromatin modification, leukaemia and implications for therapy. Br J Haematol 2002;118:714–27.

6. Bakkenist CJ, Kastan MB. DNA damage activates ATM through intermolecular autophosphorylation and dimer dissociation. Nature 2003;421:499–506.

7. Ju R, Muller MT. Histone deacetylase inhibitors activate p21(WAF1) expression via ATM. Cancer Res 2003;63:2891–7.

8. Gottlicher M, Minucci S, Zhu P, et al. Valproic acid defines a novel class of HDAC inhibitors inducing differentiation of transformed cells. EMBO J 2001;20:6969–78.

9. Amin HM, Saeed S, Alkan S. Histone deacetylase inhibitors induce caspase-dependent apoptosis and downregulation of daxx in acute promyelocytic leukaemia with t(15;17). Br J Haematol 2001;115:287–97.

10. Nebbioso A, Clarke N, Voltz E, et al. Tumor-selective action of HDAC inhibitors involves TRAIL induction in acute myeloid leukemia cells. Nat Med 2005;11:77–84.

11. Insinga A, Monestiroli S, Ronzoni S, et al. Inhibitors of histone deacetylases induce tumor-selective apoptosis through activation of the death receptor pathway. Nat Med 2005;11:71–6.

12. Rogakou EP, Pilch DR, Orr AH, Ivanova VS, Bonner WM. DNA double-stranded breaks induce histone H2AX phosphorylation on serine 139. J Biol Chem 1998;273:5858–68.

13. Thiriet C, Hayes JJ. Chromatin in need of a fix: phosphorylation of H2AX connects chromatin to DNA repair. Mol Cell 2005;18:617–22.

14. Jeggo PA. DNA double strand breakage and repair. In: Hall JC, Dunlap JC, Friedmann T, Gianelli F, editors. Advances in Genetics. Philadelphia: Academic Press Inc. 1998;38:185–218.

15. Raderschall E, Golub EI, Haaf T. Nuclear foci of mammalian recombination proteins are located at single-stranded DNA regions formed after DNA damage. Proc Natl Acad Sci U S A 1999;96:1921–6.

16. Brady N, Gaymes TJ, Cheung M, Mufti GJ, Rassool FV. Increased error-prone NHEJ activity in myeloid leukemias is associated with DNA damage at sites that recruit key nonhomologous end-joining proteins. Cancer Res 2003;63:1798–805.

17. Rassool FV, North PS, Mufti GJ, Hickson ID. Constitutive DNA damage is linked to DNA replication abnormalities in Bloom's syndrome cells. Oncogene 2003;22:8749–57.

18. Fernandez-Capetillo O, Celeste A, Nussenzweig A. Focusing on foci: H2AX and the recruitment of DNA-damage response factors. Cell Cycle 2003;2:426–7.

19. Sedelnikova OA, Pilch DR, Redon C, Bonner WM. Histone H2AX in DNA damage and repair. Cancer Biol Ther 2003;2:233–5.

20. Brown D, Kogan S, Lagasse E, et al. A PMLRARα transgene initiates murine acute promyelocytic leukemia. Proc Natl Acad Sci U S A 1997;94:2551–6.

21. Lallemand-Breitenbach V, Guillemin MC, Janin A, et al. Retinoic acid and arsenic synergize to eradicate leukemic cells in a mouse model of acute promyelocytic leukemia. J Exp Med 1999;189:1043–52.

22. Zhu J, Lallemand-Breitenbach V, de The H. Pathways of retinoic acid- or arsenic trioxide-induced PML/RARα catabolism, role of oncogene degradation in disease remission. Oncogene 2001;20:7257–65.

23. Lallemand-Breitenbach V, Zhu J, Puvion F, et al. Role of promyelocytic leukemia (PML) sumolation in nuclear body formation, 11S proteasome recruitment, and As_2O_3-induced PML or PML/retinoic acid receptor α degradation. J Exp Med 2001;193:1361–71.

24. Paull TT, Rogakou EP, Yamazaki V, Kirchgessner CU, Gellert M, Bonner WM. A critical role for histone H2AX in recruitment of repair factors to nuclear foci after DNA damage. Curr Biol 2000;10:886–95.

25. Celeste A, Difilippantonio S, Difilippantonio MJ, et al. H2AX haploinsufficiency modifies genomic stability and tumor susceptibility. Cell 2003;114:371–83.

26. Malumbres M, Hunt SL, Sotillo R, et al. Driving the cell cycle to cancer. Adv Exp Med Biol 2003;532:1–11.

27. Glaser KB, Staver MJ, Waring JF, Stender J, Ulrich RG, Davidsen SK. Gene expression profiling of multiple histone deacetylase (HDAC) inhibitors: defining a common gene set produced by HDAC inhibition in T24 and MDA carcinoma cell lines. Mol Cancer Ther 2003;2:151–63.

28. Waxman S, Huang Y, Scher BM, Scher M. Enhancement of differentiation and cytotoxicity of leukemia cells by combinations of fluorinated pyrimidines and differentiation inducers: development of DNA double-strand breaks. Biomed Pharmacother 1992;46:183–92.

29. Kovacs JJ, Murphy PJ, Gaillard S, et al. HDAC6 regulates Hsp90 acetylation and chaperone-dependent activation of glucocorticoid receptor. Mol Cell 2005;18:601–7.

30. Ayton PM, Cleary ML. Molecular mechanisms of leukemogenesis mediated by MLL fusion proteins. Oncogene 2001;20:5695–707.

31. Ungerstedt JS, Sowa Y, Xu WS, et al. Role of thioredoxin in the response of normal and transformed cells to histone deacetylase inhibitors. Proc Natl Acad Sci U S A 2005;102:673–8.

32. Rahmani M, Reese E, Dai Y, et al. Coadministration of histone deacetylase inhibitors and perifosine synergistically induces apoptosis in human leukemia cells through Akt and ERK1/2 inactivation and the generation of ceramide and reactive oxygen species. Cancer Res 2005;65:2422–32.

33. Early A, Drury LS, Diffley JF. Mechanisms involved in regulating DNA replication origins during the cell cycle and in response to DNA damage. Philos Trans R Soc Lond B Biol Sci 2004;359:31–8.

34. Weinreich M, Palacios DeBeer MA, Fox CA. The activities of eukaryotic replication origins in chromatin. Biochim Biophys Acta 2004;1677:142–57.

35. Fanidi A, Harrington EA, Evan GI. Cooperative interaction between c-myc and bcl-2 proto-oncogenes. Nature 1992;359:554–6.

36. Omidvar N, Pearn L, Burnett AK, Darley RL. Ral is both necessary and sufficient for the inhibition of myeloid differentiation mediated by Ras. Mol Cell Biol 2006;26:3966–75.

AACR American Association for Cancer Research

Molecular Cancer Research

Histone Deacetylase Inhibitors (HDI) Cause DNA Damage in Leukemia Cells: A Mechanism for Leukemia-Specific HDI-Dependent Apoptosis?

Terry J. Gaymes, Rose Ann Padua, Marika Pla, et al.

Mol Cancer Res 2006;4:563-573. Published OnlineFirst July 28, 2006.